Biochimica et Biophysica Acta, 419 (1976) 19–41

BBA 77164

STRUCTURAL AND DYNAMICAL STUDIES OF MIXED CHLOROPHYLL/PHOSPHATIDYLCHOLINE BILAYERS VIA X-RAY DIFFRACTION, ABSORPTION POLARIZATION SPECTROSCOPY AND NUCLEAR MAGNETIC RESONANCE

F. PODO*, J. E. CAIN and J. K. BLASIE

Department of Biophysics and Physical Biochemistry, Johnson Research Foundation, University of Pennsylvania, Philadelphia, Pa. (U.S.A.)

(Received February 4th, 1975)
(Revised manuscript received June 30th, 1975)

SUMMARY

The structure and dynamics of phosphatidylcholine bilayers containing chlorophyll were studied by X-ray diffraction and absorption polarization spectroscopy in the form of hydrated orientated multilayers below the thermal phase transition of the lipid chains and by nuclear magnetic resonance in the form of single-wall vesicles above the thermal transition. Our results show that (a) chlorophyll is incorporated into the phosphatidylcholine bilayers with its porphyrin ring located anisotropically in the polar headgroup layer of the membrane and with its phytol chain penetrating in a relatively extended form between the phosphatidylcholine fatty acid chains in the hydrocarbon core of the mixed bilayer membrane and (b) the intramolecular anisotropic rotational dynamics of the host phosphatidylcholine molecules are significantly perturbed upon chlorophyll incorporation into the bilayer at all levels of the phosphatidylcholine structure. These dynamics for the host phosphatidylcholine fatty acid chains are qualitatively different from that of the incorporated chlorophyll phytol chains on a 10^{-9}–10^{-10} s time scale in the ideally mixed two-component bilayer.

INTRODUCTION

Structural and dynamical studies of lipid bilayers containing chlorophyll represent one step in a series of studies directed toward the investigation of the mechanism of energy transfer from antenna chlorophyll to reaction-center chlorophyll and the mechanism of light-induced electron transfer reactions in model membranes. The two-component bilayers were studied by X-ray diffraction and absorption polarization spectroscopy in the form of hydrated oriented multilayers below the

* On leave from the Istituto Superiore di Sanità, Physics Laboratory, Rome, Italy.

thermal phase transition of the lipid fatty-acid chains. The dynamics of these two-component bilayers were studied by pulse Fourier transform nuclear magnetic resonance (NMR) in the form of single-wall bilayer vesicles above the thermal phase transition of the chains. These studies concern the precise location of the chlorophyll molecules in the host phosphatidylcholine bilayer, the orientation of the porphyrin ring of the chlorophyll relative to the lipid bilayer, and the intramolecular rotational dynamics of the host phosphatidylcholine and the incorporated chlorophyll in the mixed bilayer model membrane.

These studies have been briefly reported elsewhere [1, 2].

MATERIALS AND METHODS

Synthetic β-γ-dipalmitoyl L-α-phosphatidylcholine and phytol were purchased from Calbiochem.

^2H_2O (99.8 %) was purchased from Thomson and Packard.

Methanol, light petroleum (30–60 °C boiling range), ethyl ether and all other reagents were reagent grade and used without further purification.

Bacteriochlorophyll was extracted in the dark and at 0–5 °C from bacteria *Rhodopseudomonas sphaeroides* (green carotenoidless mutant) and *Chromatium* after the procedure described by Smith and Benitez [3] for bacteria *Rhodospirillum Rubrum*, as modified by T. Kihara (Kihara, T., personal communication). The bacteria cells were centrifuged for 10 min at 2 °C and 5000 rev./min from their culture medium (6 bottles 0.25 gallon each, 30 h old). The wet residue was suspended in 40 ml of methanol and kept about 45 min in the refrigerator at 5 °C. A 10 min centrifugation at 15 000 rev./min was then carried out and the light brown supernatant discarded. The procedure was repeated three times and the dark green supernatants obtained by means of the second and third centrifugations were combined (about 80 ml) in a 125 ml separating funnel. About 10 ml of light petroleum and about 5 ml of distilled water were added to the methanol solution. The vigorously stirred suspension was allowed to separate. The upper light petroleum phases from two successive extractions were collected, combined and their volume reduced by aspiration. The material was then placed on a Baker aluminium oxide column (1 cm diameter, about 25 cm high) which had been previously washed with light petroleum. The column, developed with light petroleum at low temperature, was finally eluted with light petroleum containing increasing amounts of ethyl ether (starting with an ethyl ether volume fraction of 3 %, up to about 20 %). The yellow-orange carotenoid fraction and the blue-green pigments (chlorophyll) were collected in series. The chlorophyll fraction, freed of the light petroleum/ethyl ether solution under reduced pressure, was finally dissolved in ethyl ether and kept below 0 °C.

The bacteriochlorophyll purity was determined by analysing the absorption spectrum between 350 and 800 nm [3, 4] by means of a Perkin Elmer Coleman 124 split-beam spectrophotometer. The A_{391}/A_{577} and the A_{358}/A_{577} ratios corresponded to within about 5 % of the values reported by Smith and Benitez [3]. A shoulder at 435 nm indicated the possible presence of a small trace of greenish or gray-blue fractions [4], corresponding to oxidized components of bacteriochlorophyll. Quantitative estimations of the pigment concentration were carried out using the Beer-Lambert Law:

$A(\lambda) = \alpha(\lambda) \cdot Mdc$

where d is the pathlength within the solution, $\alpha(\lambda)$ the specific absorption coefficients, M its molecular weight, and c the concentration in mol/l. The absorption coefficient $\alpha(577) = 22.9$ was used according to the data of Smith and Benitez [3].

Purified chlorophyll *a* from spinach was purchased from Sigma Chemical Company, supplied in a sealed ampoule and stored in the dark below 0 °C. The purity of the pigment (declared substantially free of chlorophyll *b*) was checked by analysing its optical absorption spectrum in ethyl ether. In particular the A_{428}/A_{662} ratio corresponded to the value of 1.30 derived from the data of Smith and Benitez [3] for highly purified chlorophyll *a*. The values of the absorption coefficients at the two wavelengths are however about 10 % lower than those reported in ref. 3. Impurities due to pheophytin, if any, are limited; interpreting the weak absorption signal observed at 505 nm as pheophytin, its amount would be at most 10 % of the total pigment. Concentration determinations were made using the absorption coefficients given by the supplier: $E_{662} = \alpha\,(662) \cdot M = 8 \cdot 10^4$.

[^{2}H]Chlorophyll *a* was a gift of J. J. Katz (Argonne National Laboratory). The purity of the material was checked spectrophotometrically and concentrations measured in ethyl ether, usng the value of α (662) = 100.9 reported by Smith and Benitez for unlabeled chlorophyll *a* [3].

Single-wall bilayer vesicles for the X-ray diffraction experiments composed of dipalmitoyl phosphatidylcholine/bacteriochlorophyll at molar ratios of 2.3:1 and 4.6:1 were prepared in 0.015 M phosphate buffer, pH 7.5, according to the method to be described in detail for the NMR experiments. X-ray diffraction patterns for the single-wall vesicular dispersions were obtained at 20 °C, below the thermal phase transition of the lipid fatty-acid chains, according to methods described in detail previously [5–7]. Oriented multilayers for the X-ray diffraction experiments were formed from these aqueous dispersions of vesicles by partial drying at constant relative humidity on a simply curved 1 cm × 1 cm clean glass surface of radius 25 mm. X-ray diffraction patterns from the hydrated oriented multilayers maintained at constant temperature (20 °C) and various relative humidities were obtained with modified Frank's cameras using either line-focus or point-focus and grazing incidence according to procedures described in detail previously [5–7].

Hydrated oriented multilayers with an area of 1 cm × 1.5 cm for the absorption polarization spectra were prepared on planar glass cover slips in a manner similar to that described for the X-ray diffraction experiments. Spectra were recorded from 300 nm to 850 nm with a Cary 14 split-beam spectrophotometer utilizing a dipalmitoyl phosphatidylcholine multilayer specimen in the reference beam and a dipalmitoyl phosphatidylcholine chlorophyll multilayer specimen of approximately equal thickness in the measuring beam as a function of the polarization of the beams (0° and 90° relative to the specimen rotation axis) at a fixed angle of incidence of the beams on the specimens (45° or 60°). Polarization and incidence conditions were identical in each beam to about one degree.

Vesicles for the NMR experiments composed of dipalmitoyl phosphatidylcholine/bacteriochlorophyll at a molar ratio 4.5:1 (phosphatidylcholine (25 mM), dipalmitoyl phosphatidylcholine/chlorophyll *a* 3:1 (phosphatidylcholine 26 mM), dipalmitoyl phosphatidylcholine/[^{2}H]chlorophyll *a* 3:1 (phosphatidylcholine 18 mM)

were prepared in aqueous dispersions according to the following procedure. Ethyl ether was evaporated from the chlorophyll in the dark under reduced pressure. The pigments were dissolved in methanol and the phosphatidylcholine was added. The solvent was evaporated by means of N_2 gas flow, and the dry residue suspended in a ^2H_2O solution containing 45 mM NaCl, 30 mM sodium acetate and 5 mM sodium phosphate. Vesicles were prepared by low-power sonication of the suspension, performed under N_2 in the dark, above the thermal phase transition temperature of the chains, with a Sonifier Cell Disruptor Model W 185 (Ultrasonics, Inc.). Periods of 30 s sonication were alternated with intervals sufficient to restore thermal equilibrium in the sample. The total time of sonication was typically 5 min. An analogous procedure was followed for the dipalmitoyl phosphatidylcholine/phytol sample, prepared at a molar ratio 2:1 (phosphatidylcholine 18 mM). After the transfer to 5 mm diameter NMR tubes, the samples were degassed and kept under argon. During the time required for the NMR experiments (typically the order of one day) the samples were maintained above the thermal phase transition. In the intervals required for allowing the NMR probe to attain thermal equilibrium at the working temperature, the sample was maintained at about 60 °C by a separate bath. The measurements were started at least 30 min after the transfer of the sample into the probe. This procedure was used to minimize or to avoid possible temperature hysteresis effects in the samples. Spin-lattice relaxation times (T_1) appeared unaltered upon repeating experiments on the samples containing unlabeled chlorophyll *a* and [^{2}H]chlorophyll *a* kept for a few days at room temperature. When NMR measurements required more than one day for the same sample, the independence of the spin-lattice relaxation times and resonance linewidths on further sonication and sample aging was also checked. The T_1 values and linewidths were required to be unaltered by a new 2 min sonication.

NMR spectra and pulsed NMR measurements of spin-lattice relaxation times [8, 9] for individual protons in the phospholipid bilayers were performed at 220 MHz using a Varian HR-220 spectrometer equipped with a frequency sweep unit and a Varian model V-4340 variable temperature accessory. A Varian 620-I computer was used to control the widths and timing of the transmitter radio-frequency pulses and to collect the free induction decay signals from the receiver, after an appropriate sequence of pulses. The employed pulse-sequence was ($\pi/2$, homospoil, τ, $\pi/2$, free induction decay, homospoil) [10]. The pulse sequence and the collection of data could be repeated and accumulated as many times as necessary for a given delay time τ in order to achieve the desired signal-to-noise ratio [9]. The partially relaxed spectra in the frequency domain were calculated by applying the Fourier transform operation to the free induction decay signals by means of the 620-I computer [8]. The T_1 value of each individual line was determined by a computer analysis through a best fit procedure applied to the line intensities of the partially relaxed spectra as functions of delay time τ [10]. Peak areas have been evaluated by weight.

All calculations were performed on the PDP-10 computer of the University of Pennsylvania Medical School Computer Facility.

RESULTS AND ANALYSIS

Intensity data for a single-wall vesicular dispersion of dipalmitoyl phos-

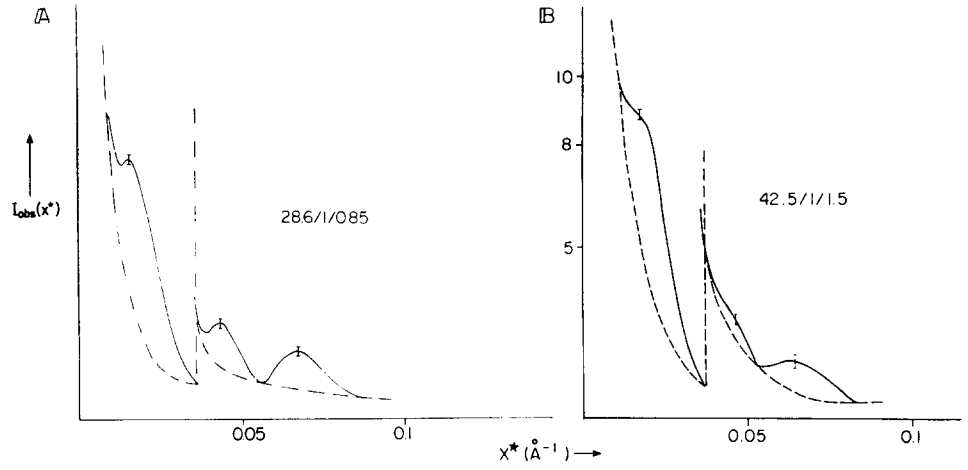

Fig. 1. Low-angle X-ray intensity data $I(x^*)$ obtained from single-wall vesicular dispersions of dipalmitoyl phosphatidylcholine (A) and dipalmitoyl phosphatidylcholine/bacteriochlorophyll (2.3 : 1) (B) $x^* = (2\sin\theta)/\lambda$. The relative intensities of the three maxima are indicated in the figure for each case.

TABLE I

h^2I (h/d) DATA

h	Dipalmitoyl phosphatidylcholine/bacteriochlorophyll (2.3 : 1)			Dipalmitoyl phosphatidylcholine/bacteriochlorophyll (4.6 : 1)		Estimated error in measured integrated intensities before scaling
	15 % (d = 56.5 Å)	31 % (d = 57.5 Å)	56 % (d = 58.5 Å)	15 % (d = 55.0 Å)	31 % (d = 55.9 Å)	
1	0.615*	0.546*	0.402*	0.497*	0.448*	±7 %
2	0.002	~0	0.010	0.002	0.001	±7 %
3	0.002	0	0.011	0.004	~0	±8 %
4	0.255	0.310	0.429	0.309	0.397	±9 %
5	0	0.004	0.004	0.001	0.003	±4 %
6	0.042	0.079	0.086	0.062	0.063	±7 %
7	0	0	0	0	0	
8	0.036	0.053	0.056	0.068	0.063	±6 %
9	0.020	0.009	–	0.023	0.016	±4 %
10	0.028	–	–	0.034	0.009	±4 %

* Before absorption correction.

phatidylcholine/bacteriochlorophyll at a molar ratio of 2.3:1 at 20 °C is shown in Fig. 1 and is similar to that obtained for dipalmitoyl phosphatidylcholine alone as described by us previously [7].

The integrated intensities for the lamellar reflections from hydrated oriented multilayers of these same bilayers at 20 °C and several relative humidities are given

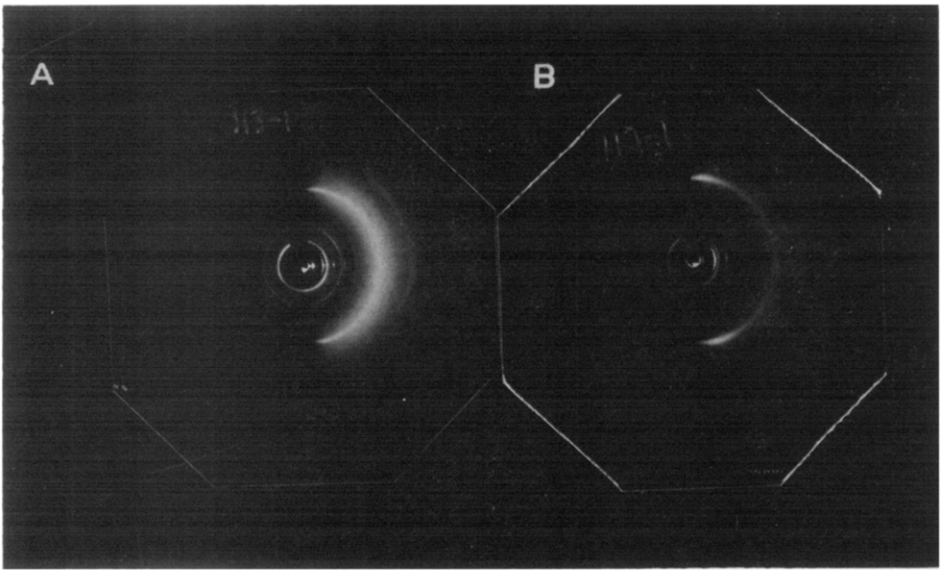

Fig. 2. Point-focus wide-angle X-ray diffraction patterns from hydrated oriented multilayers of dipalmitoyl phosphatidylcholine (B) and dipalmitoyl phosphatidylcholine/bacteriochlorophyll (2.3:1) (A). The lamellar reflections occur only along the positive horizontal axis due to absorption by the glass substrate. For dipalmitoyl phosphatidylcholine, the near equatorial diffraction from the packing of fatty acid chains in the plane of the bilayer occurs predominately at right angles to the lamellar reflections at $x^* \simeq \pm 1/4.15$ Å. The corresponding diffraction for the dipalmitoyl phosphatidylcholine/bacteriochlorophyll occurs at $x^* \simeq \pm 1/4.25$ Å with considerable off-equatorial spreading even though these bilayers are as well oriented as the dipalmitoyl phosphatidylcholine bilayers. The complete diffraction rings arise from the windows on the specimen chamber, the first of which falls just outside the fourth order lamellar reflection in both cases.

in Table 1. The unit cell dimension d along the axis normal to the plane of the multilayer, the estimated error in the integrated intensities and the relative humidities are indicated in this table.

Point-focus wide-angle diffraction patterns from hydrated oriented multilayers of dipalmitoyl phosphatidylcholine and dipalmitoyl phosphatidylcholine/bacteriochlorophyll at a molar ratio of 2. 3:1 at 20 °C are shown in Fig. 2.

It has been shown by us that the diffracted X-ray intensities from dispersions of single-wall vesicles of lipids are, to a good approximation, proportional to the spherically averaged absolute square of the continuous Fourier transform $|F(x)^*|^2$, of the electron density profile of a lipid bilayer $\mu(x)$ (the electron density distribution of the bilayer projected onto an axis x, normal to the plane of the bilayer) [5–7, 11]. An integral Fourier transformation of the corrected intensity data from dispersions provides the Patterson function for the bilayer profile, $P_0(x) = \mu(x) * \mu(-x)$ (* stands for convolution). $\mu(x)$ can then be obtained directly by a convolution square root of $P_0(x)$ [5–7]. The derived $\mu(x)$ determines the value of the phase angle within each maximum of $|F(x^*)|^2$ observed in diffraction from dispersions. These phase angles for the first three maxima of $|F(x^*)|^2$ are typically π, 0, π, respectively, for intensity data similar to that shown in Fig. 1 [7].

The corrected* relative intensities of the lamellar reflections from oriented multilayers are proportional to the value of $|F(x^*)|^2$ sampled at the reciprocal lattice points, $x^* = h/d$. Lamellar reflections from multilayers can be observed to considerably higher diffraction angles than can $|F(x)^*|^2$ from dispersions. Therefore, $\mu(x)$ can be calculated to higher resolution with multilayer data if the phases of the reflections can be determined. The phases of the first 3–4 reflections are known since they occur within the observed maxima from dispersions, and these reflections fit onto the continuous $|F(x^*)|^2$ obtained from dispersions [7]. In order to determine the phases of the higher-order reflections ($h > 4$), we use the Fourier sampling theorem [30] to reconstruct a continuous $F(x^*)$ from sampled $|F(h/d)|$ data from multilayers. The sampling theorem may be written:

$$F(x^*) = \sum_{h=-h_{max}}^{+h_{max}} |F(h/d)| \exp[-i\phi(h)] \operatorname{sinc}[\pi(x^*d - h)]$$

where $\phi(h)$ is the phase of the reflection of order h. h_{max} is the highest-order reflection observed. The structure of the bilayer will be nearly the same if the multilayers are allowed to swell from a spacing d to a slightly different spacing d'. If the phases of the first few reflections are known from dispersion data, it may be found that only one of the possible combinations of ϕ (h) for $4 < h \leqslant h_{max}$ results in a reconstructed $|F(x^*)|^2$ such that the reflections $|F(h/d)|^2$ and $|F(h/d')|^2$ fit on the same continuous $|F(x^*)|^2$ in the region $4/d \leqslant x^* \leqslant h_{max}/d$. All other phase combinations for $h = 5 \rightarrow h_{max}$ should then result in reconstructions that violate either the sign or magnitude of the observed $\{|F(h/d)|^2 - |F(h/d')|^2\}$ for $h = 5 \rightarrow h_{max}$ [7]. Generally, the smaller $(d' - d)$, the better the observed $|F(h/d)|^2$ and $|F(h/d')|^2$ will fit on the same $|F(x^*)|^2$. Some of the $\{|F(h/d)|^2 - |F(h/d')|^2\}$ must be larger than the experimental error in the intensities for $x^* > 4/d$. Otherwise, $(d' - d)$ can be small and changes in the period of 1–2 Å are sufficient for this phasing procedure.

$|F(0/d)|^2$ was not observed. It is, however, required in the reconstruction of $F(x^*)$. Values for $F(0/d)$ may be arbitrarily chosen such that $\mu(x)$ calculated by a continuous Fourier transformation of reconstructed $F(x^*)$ that started at the first zero of $F(x^*)$ and extended to $x^* = (h_{max}+1)/d$ is nearly identical to that $\mu(x)$ calculated by a conventional Fourier synthesis with the same phase combination for $h = 1 \rightarrow h_{max}$. $|F(0/d)|^2$ determined in this manner for such multilayer systems is generally small compared to the higher orders [7]. Hence, any uncertainty in $|F(0/d)|$ cannot significantly affect $F(x^*)$ for $x^* > 4/d$ or the phases $\phi(h)$ for $h = 5 \rightarrow h_{max}$. $\mu(x)$ was then calculated by a Fourier transformation of this reconstructed $F(x^*)$ with the correct phases. Calculations of $\mu(x)$ in this manner avoids transform truncation artifacts in the region of $x \simeq \pm d/2$, where $x = 0$ is taken as the center of the lipid bilayer. It is important to note that the effect of errors in the observed intensities of the lamellar reflections on the determination of the phases is immediately apparent, even for the weaker reflections, when this phasing procedure is used.

---

* The integrated intensities of the observed lamellar reflections $I(h)$ from the multilayer must be corrected by a factor of h^2 because of the curvature of the multilayer specimen and for imperfect orientation of the lamellae, and for absorption. The latter is determined for the lower order lamellar reflections (meridional) from the corresponding decrease due to absorption in the diffracted intensity from the lipid hydrocarbon chains on approaching the equator.

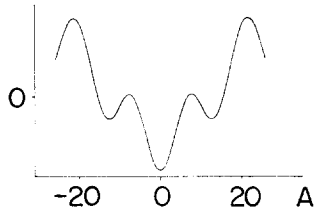

Fig. 3. Low-resolution relative electron density profile $\mu(x)$ obtained by the convolution square-root of $P_0(x)$. The zero level represents to good approximation the average electron density of the aqueous medium in the case of these vesicular dispersions.

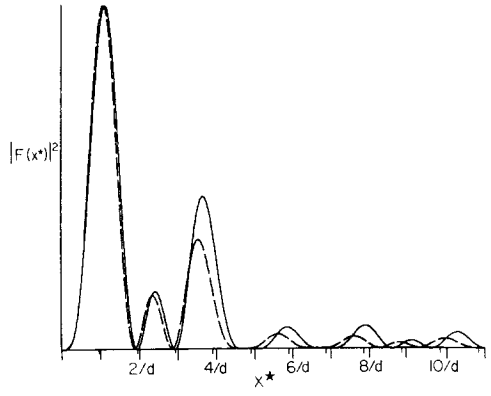

Fig. 4. Continuous $|F(x^*)|^2$ reconstructed with ten orders of lamellar diffraction from dipalmitoyl phosphatidylcholine/bacteriochlorophyll multilayers at phosphatidylcholine/bacteriochlorophyll ratios of 2.3 : 1 (- - -) and 4.6 : 1 (—).

This is not the case after the intensity data has been subjected to a Fourier transformation. This phasing procedure has been described previously by us [7].

Fig. 3 shows the low-resolution electron density profile structure $\mu(x)$ obtained by the convolution square root of the $P_0(x)$ obtained from such data as that in Fig. 1. It may be noted that $-\mu(x)$ is also a convolution square root of $P_0(x)$. However, the negative of $\mu(x)$ cannot represent a physically viable profile structure for a single lipid bilayer surrounded by an aqueous medium. Reconstructed $|F(x^*)|^2$ for the two bilayers dipalmitoyl phosphatidylcholine/bacteriochlorophyll at molar ratios of 4. 6:1 and 2. 3:1 at 15 % relative humidity are shown in Fig. 4 in the region $0.5\ d \leqslant x^* \leqslant 11/d$. All reflections $-10 \leqslant h \leqslant +10$ were used in the reconstruction. Higher-order lamellar reflections were not observed and hence these reconstructions should be accurate even near $x^* \approx 10/d$. It should be noted that these reconstructed $|F(x^*)|^2$ also fit the available $\{|F(h/d)|^2 - |F(h/d')|^2\}$ lamellar reflection data for $h = 1 \rightarrow 4$. Hence, the reconstruction of $|F(x^*)|^2$ can be used in these two cases to phase all the lamellar reflections for $h = 1 \rightarrow 10$. The corresponding high-resolution electron density profile structure $\mu(x)$ for these two bilayers at 6 Å resolution are shown in Fig. 5 together with their difference profile structure $\Delta\mu(x)$.

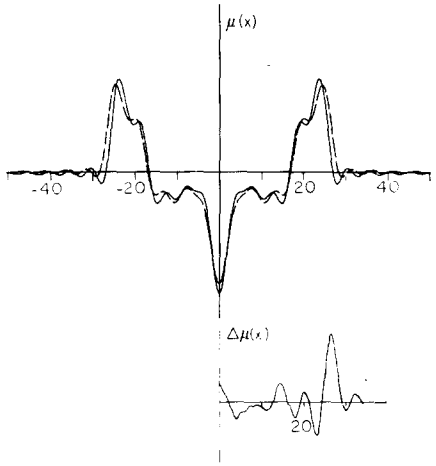

Fig. 5. 6 Å-resolution relative electron density profiles $\mu(x)$ for two dipalmitoyl phosphatidylcholine bacteriochlorophyll bilayers at dipalmitoyl phosphatidylcholine : bacteriochlorophyl lratios of 2.3 : 1 (- - -) and 4.6 : 1 (—). Their difference profile $\Delta\mu(x)$ is also shown. The abscissae are marked at intervals of 10 Å.

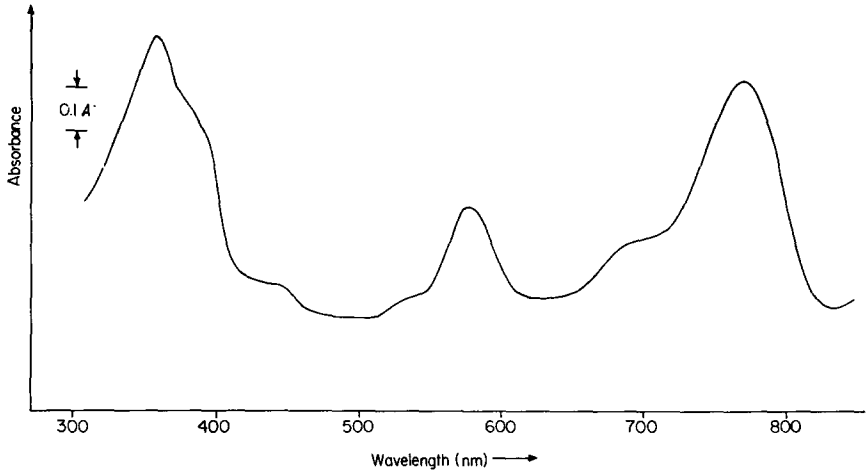

Fig. 6. Absorption spectrum for bacteriochlorophyll in a hydrated multilayer of dipalmitoyl phosphatidylcholine/bacteriochlorophyll (2.3 : 1).

The absorption spectra for bacteriochlorophyll in a hydrated oriented dipalmitoyl phosphatidylcholine/bacteriochlorophyll multilayer is shown in Fig. 6. The absorption of the 360 nm and 770 nm transitions as a function of polarization and angle incidence are given in Table II. The absorption ratios for the two transitions as a function of polarization were analyzed according to the theory developed independently by us and it is similar to that described in ref. 23. The 360 nm and 770 nm transitions were found to be inclined 55.5° and 55°, respectively, to the normal of the plane of the bilayer, and therefore the porphyrin ring is inclined 54° to the bilayer below the thermal phase transition of the lipid fatty-acid chains. These results

TABLE II

POLARIZED ABSORPTION DATA

Wavelength	Incident angle	Polarization angle	Dipalmitoyl phosphatidylcholine/bacteriochlorophyll multilayer absorbance				
			2.3 : 1	4.6 : 1	4.6 : 1	23 : 1	23 : 1
Blue	45°	0°	0.645	0.670	1.320	1.601	1.250
(360 nm)	45°	90°	0.625	0.659	1.167	1.542	1.225
	60°	0°	0.647	0.569	1.130	1.578	1.320
	60°	90°	0.635	0.543	1.048	1.574	1.315
Red	45°	0	0.500	0.490	0.980	1.268	1.063
(770 nm)	45°	90°	0.493	0.490	0.930	1.229	1.043
	60°	0°	0.494	0.400	0.860	1.258	0.992
	60°	90°	0.496	0.400	0.850	1.263	1.047

are independent of the bacteriochlorophyll concentration in the bilayer for molar ratios of dipalmitoyl phosphatidylcholine/bacteriochlorophyll of 2.3:1–23:1.

The PMR CW spectrum at 220 MHz of phytol (37 mM) in C^2HCl_3 is shown in Fig. 7. Peak assignments for phytol are in agreement with those reported in the Varian spectra catalog (1962) [12]. The resonances of (a) and (b) side-chain methyl groups on saturated carbons atoms are centered at the same resonance frequency as the terminal methyl groups of dipalmitoyl phosphatidylcholine fatty acid chains (9.13 ppm). The coincidence is retained in the sonicated dipalmitoyl phosphatidylcholine/ phytol vesicles (Fig. 8). The same consideration holds for the methylene groups along the phytol structure that are sufficiently far from the isoprenoid unit double bond as to be unaffected by its magnetic anisotropy. The methylene groups on the reduced isoprenoid units, (most likely coincident with the -C-H protons)

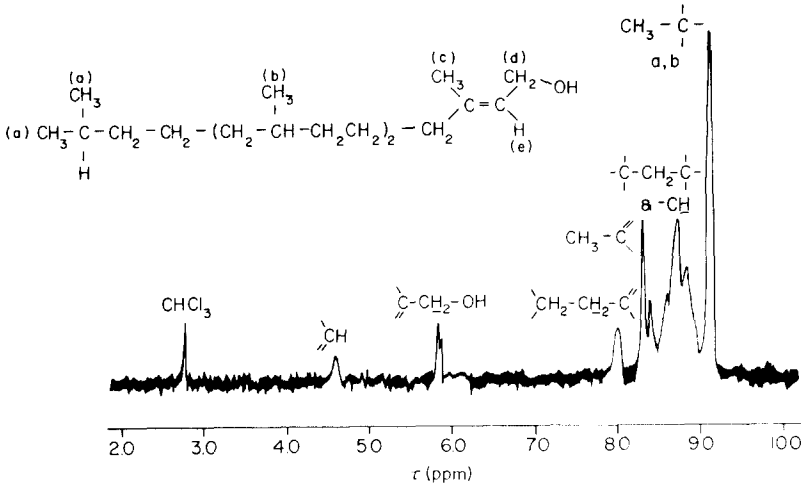

Fig. 7. PMR spectrum (CW) at 220 MHz of 37 mM phytol in C^2HCl_3. Peak assignments are indicated.

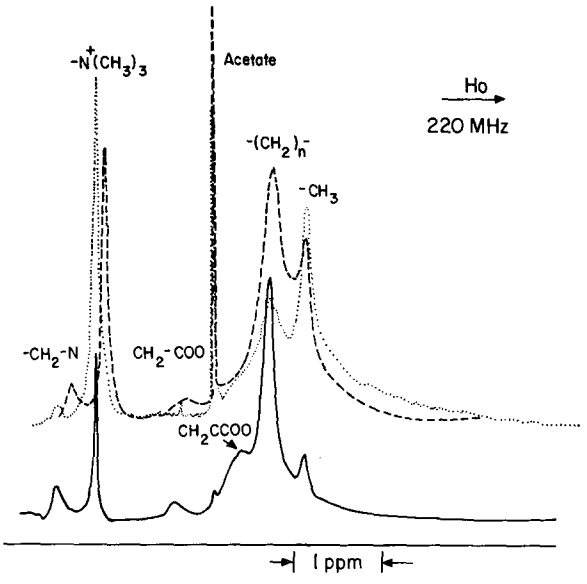

Fig. 8. PMR spectrum (FT) at 220 MHz of dipalmitoyl phosphatidylcholine (—), dipalmitoyl phosphatidylcholine/phytol (2 : 1) (...) and dipalmitoyl phosphatidylcholine /[^{2}H]chlorophyll *a* (3 : 1) (- - -) vesicles in aqueous solution above the thermal phase transitions of the chains. Peak assignments are indicated.

show a broad composite resonance with the maximum at 8.74 ppm. The (c)-methyl resonance appears at 8.33 ppm. This resonance position is identical to that of the methyl resonances in geraniol [12] and, according to the Bates and Gale peak assignments in trisubstituted double bonds in terpenoids [13], suggests that the methyl groups are in the *trans* conformation with respect to the CH group in the isoprenoid unit. The chemical shifts of the allylic methylene doublet = C-CH_2-OH and of the vinyl proton (= CH) in the isoprenoid unit are respectively 5.85 and 4.59 ppm, in agreement with the literature data [12]. The peak at 8 ppm is attributed to the methylene -C-CH_2-C = , connecting the isoprenoid and reduced isoprenoid units, in agreement again with peak assignments in geraniol [12]. The peak areas, as obtained by graphical analysis and weighting the partially overlapping bands, support the mentioned assignments. The peak at 8.40 ppm, due to two protons, is tentatively attributed to the -C-CH_2-C-C = groups.

In the PMR FT spectra of dipalmitoyl phosphatidylcholine/phytol vesicles (Fig. 8), the only resonances that could be clearly resolved from the noise, even with the help of the Fourier transform techniques, were those of the dipalmitoyl phosphatidylcholine $N^+(CH_3)_3$ and NCH_2 and the dipalmitoyl phosphatidylcholine and phytol chains' methylene and methyl groups bonded to saturated carbon atoms. The other resonances from phytol are either broadened or obscured by the broadened dipalmityol phosphatidylcholine resonances.

The PMR CW spectrum of bacteriochlorophyll in C^2HCl_3 shows a sharp resonance due to methylene groups on saturated carbons ($\Delta\nu_{\frac{1}{2}}$ = 6 Hz) with the typical doublet [14] of the methyl resonances from isopropyl and reduced isoprenoid

units, observed with phytol. The area ratio of the paraffinic methylene and methyl groups is in agreement (within 10 %) with the presence of a phytyl side-chain esterifying this bacteriochlorophyll at the propionic acid level. A broad and composite resonance band is observed, centered at the position 8.43 ppm. This band should comprise, in addition to the methyl group on the isoprenoid unit and the methylene $-CH_2-C-C=$, the two methyl groups from the porphyrin ring [15, 16]. The area ratio of this band to that of the paraffinic methyl resonances is about 1, in agreement with this assignment. No water resonance was detected in the spectrum of 8 mM bacteriochlorophyll in C^2HCl_3: the experimental conditions of signal-to-noise were such that any water concentration larger than 1 mM and giving a sharp resonance would be detected.

In Fig. 8 the PMR FT spectrum of dipalmitoyl phosphatidylcholine vesicles in aqueous solution is compared with those of dipalmitoyl phosphatidylcholine/phytol and dipalmitoyl phosphatidylcholine/[^{2}H]chlorophyll *a*, above the thermal phase transition of the chains. Chemical shifts and resonance linewidths of dipalmitoyl phosphatidylcholine/chlorophyll and dipalmitoyl phosphatidylcholine/ bacteriochlorophyll resonances appeared the same in the three systems incorporated with chlorophylls, provided that analogous conditions of sonication were applied. While the introduction of phytol into the dipalmitoyl phosphatidylcholine bilayer does not modify the chemical shift of any phosphatidylcholine proton resonance resolved from the noise, chlorophyll incorporation induces upfield shifts on the *N*-methyl and *N*-methylene resonance (+0.11 ppm) in the choline group. The *N*-methyl resonance is clearly composed of two neighboring peaks, still resolved at temperatures considerably higher than the chain melting point; the intensity ratio

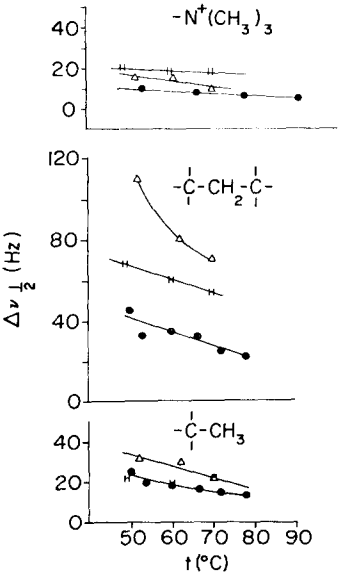

Fig. 9 Resonance linewidths $\Delta\nu_{\frac{1}{2}}$ in Hz of the main resonances in the systems dipalmitoyl phosphatidylcholine (●), dipalmitoyl phosphatidylcholine/phytol (2 : 1) (△) and dipalmitoyl phosphatidylcholine/ chlorophyll (3 : 1) (H) as a function of temperature.

of the lower to the upper-field peaks is about 1:0.65. It is worth noting that an analogous splitting of the quaternary ammonium methyl resonance has been observed in pure phosphatidylcholine vesicles as well [17, 18] at temperatures not far from the melting point and attributed to the $N^+(CH_3)_3$ resonances on the inner and outer vesicle surfaces respectively [18]. In the dipalmitoyl phosphatidylcholine/chlorophyll systems the two components are shifted in parallel to a higher field, with respect to pure phosphatidylcholine. The chemical shifts of the C_4–C_{15} methylene group resonances in the dipalmitoyl phosphatidylcholine fatty-acid chains are not substantially altered by either phytol or chlorophyll incorporation. As already mentioned, the methylene unit in the C_2 position is so much broadened upon phytol incorporation that it is practically unresolved because of the noise. In the dipalmitoyl phosphatidylcholine/chlorophyll systems, where it can still be resolved, this peak appears shifted up-field (+0.14 ppm).

The resonance linewidths of the main resonances in the systems depalmitoyl phosphatidylcholine, dipalmitoyl phosphatidylcholine/phytol and dipalmitoyl phosphatidylcholine/chlorophyll are plotted in Fig. 9 as a function of the temperature. While the linewidths of the methyl groups on the quaternary nitrogen as well as those in the alkyl chains differ in the three systems by only few Hz, the alkyl chain methylene resonances appear considerably broader in the dipalmitoyl phosphatidylcholine/phytol and dipalmitoyl phosphatidylcholine/chlorophyll systems than in pure phosphatidylcholine. It is worth noting explicitly that both the phosphatidylcholine and phytyl methylene groups contribute to this signal. The most pronounced broadening is observed in the system dipalmitoyl phosphatidylcholine/phytol, especially at lower temperatures.

Spin-lattice relaxation rates (T_1^{-1}) have been measured as a function of the temperature on the samples of dipalmitoyl phosphatidylcholine vesicles containing

TABLE III

PROTON SPIN-LATTICE RELAXATION RATES T_1^{-1} (s^{-1}) IN SONICATED VESICLES OF DIPALMITOYL PHOSPHATIDYLCHOLINE, DIPALMITOYL PHOSPHATIDYLCHOLINE/CHLOROPHYLL *a* (3 : 1) AND DIPALMITOYL PHOSPHATIDYLCHOLINE/BACTERIOCHLOROPHYLL (4.5 : 1)

	Dipalmitoyl phosphatidylcholine		Dipalmitoyl phosphatidylcholine/chlorophyll		Dipalmitoyl phosphatidylcholine/bacteriochlorophyll	
	t(°C)	T_1^{-1}(*)	*t*(°C)	T_1^{-1}*	*t*(°C)	T_1^{-1}*
$N^+(CH_3)_3$	50	1.92	49	2.16	52	3.39
	60	1.45	60	1.73	61	2.02
	70	1.08	70	1.50	71	1.04
$-\overset{\vert}{C}-CH_2-\overset{\vert}{C}-$	50	1.68	49	1.80	52	1.44
	60	1.50	60	1.54	61	1.40
	70	1.25	70	1.40	71	0.95
$-CH_3$	50	1.30	49	1.54	52	2.27
	60	0.93	60	1.24	61	1.66
	70	0.67	70	1.50	71	0.63

* Estimated experimental errors: ±5 % for $N^+(CH_3)_3$ and $C\text{-}CH_2\text{-}C$; ±20 % for CH_3.

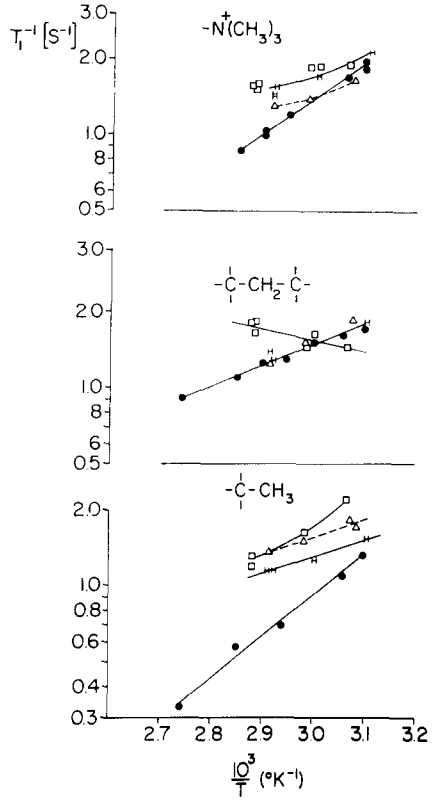

Fig. 10. Spin-lattice relaxation rates ($1/T_1$) in s^{-1} as a function of temperature for the three main resonances of the four systems dipalmitoyl phosphatidylcholine (●), dipalmitoyl phosphatidylcholine/phytol (2 : 1) (△), dipalmitoyl phosphatidylcholine/chlorophyll *a* (3 : 1) (H), dipalmitoyl phosphatidylcholine/[^{2}H]chlorophyll *a* (3 : 1) (□).

phytol, and unlabeled and ^{2}H-labeled chlorophyll *a*. The results are compared in Fig. 10 with those of pure phosphatidylcholine vesicles (the latter have been reported elsewhere) [19]. The *N*-methyl relaxation rates are only slightly affected by introduced phytol, but strongly enhanced by the presence of unlabeled chlorophyll *a* and [^{2}H]chlorophyll *a*. An accurate evaluation of the relaxation rates appeared difficult for the two individual components of the *N*-methyl signal. However, the relative ratio of their intensities was maintained essentially unaltered in the partially relaxed spectra, indicating that to a first approximation, the spin-lattice relaxation rates of the two species must be the same. The spin-lattice relaxation rates of chain methylene groups bonded to saturated carbon atoms in dipalmitoyl phosphatidylcholine/phytol and dipalmitoyl phosphatidylcholine/chlorophyll *a* are practically coincident with those found for pure phosphatidylcholine bilayers. The spin-lattice relaxation rates of the chain methylene groups measured in dipalmitoyl phosphatidylcholine/[^{2}H]chlorophyll *a* show a remarkably different behavior, characterized by a negative slope of the rate vs the reciprocal temperature. It should be kept in mind that in this system the relaxation of the chain methylene resonance band is

due only to the phosphatidylcholine chains $-(CH_2)-_{n=4-15}$ because of the incorporation of completely deuterated chlorophyll molecules into the bilayer. The spin-lattice relaxation rates measured for the CH_3 groups in the dipalmitoyl phosphatidylcholine/phytol and dipalmitoyl phosphatidylcholine/chlorophyll systems are due to terminal methyl groups of the phosphatidylcholine chains as well as to the side-chain phytyl methyl groups on saturated carbons. The resultant relaxation rates of these groups are definitely higher than those of pure dipalmitoyl phosphatidylcholine vesicles. In the dipalmitoyl phosphatidylcholine/[^{2}H]chlorophyll system, where the CH_3 resonance is due only to phosphatidylcholine chains, the relaxation rate appears systematically higher than that of pure phosphatidylcholine bilayers, while the temperature coefficient is only slightly altered.

At 70 °C the proportion of the hydrocarbon chain protons contributing to the high-resolution spectrum in pure dipalmitoyl phosphatidylcholine vesicles has been estimated from peak area measurements to be about 90 % of the corresponding proportion of the *N*-methyl protons [19]. In dipalmitoyl phosphatidylcholine/chlorophyll *a* and dipalmitoyl phosphatidylcholine/[^{2}H]chlorophyll *a*, this proportion has been evaluated to be about 68 and 58 %, respectively. The difference corresponds (to within 15 %) to all the protons of the phytyl chains whose resonances are lost upon chlorophyll deuteration. The fraction of the chain protons seen in dipalmitoyl phosphatidylcholine/phytol (about 58 %) is even lower than in dipalmitoyl phosphatidylcholine chlorophyll *a*.

The spin-lattice relaxation rates measured for the main resonances in the system dipalmitoyl phosphatidylcholine/bacteriochlorophyll are shown in Table III where they are compared with those of pure dipalmitoyl phosphatidylcholine and dipalmitoyl phosphatidylcholine/chlorophyll *a* vesicles. The T_1 relaxation rate of the *N*-methyl resonance appears more strongly enhanced by bacteriochlorophyll than by [^{2}H] chlorophyll *a*, in the range between the melting temperature of the chains and 65 °C. The T_1^{-1} values measured along the chains indicate that the average spin-lattice relaxation rate of the methylene groups is slower in dipalmitoyl phosphatidylcholine/bacteriochlorophyll than in dipalmitoyl phosphatidylcholine/chlorophyll *a* while the opposite is true for the methyl groups of the chains, at temperatures below 65 °C. The T_1 rates measured in dipalmitoyl phosphatidylcholine/bacteriochlorophyll for the resonances due to chain methyl and methylene groups bonded to saturated carbon atoms as well as those of $N^+(CH_3)_3$ are surprisingly close to those of pure dipalmitoyl systems.

DISCUSSION: X-RAY DIFFRACTION AND ABSORPTION POLARIZATION SPECTROSCOPY

The model for the location of bacteriochlorophyll in the phosphatidylcholine bilayer membrane which qualitatively best fits the difference profile structure $\Delta\mu(x)$ for the two different concentrations of chlorophyll incorporation investigated and the changes in lipid hydrocarbon chain packing in the plane of the membrane induced by increasing chlorophyll incorporation, places the chlorophyll porphyrin ring in the polar headgroup layer of the bilayer and the chlorophyll phytol chain penetrating in a relatively extended form between the phosphatidylcholine fatty-acid chains into the hydrocarbon core. Furthermore, the orientation of the porphyrin ring in

the polar headgroup layer of the bilayer is 54° to the plane of the bilayer. The basis for this model of a mixed bilayer structure is as follows.

(a) With increasing chlorophyll incorporation, the near equatorial diffraction arising from the packing of lipid hydrocarbon chains in the plane of the bilayer membrane with the chains extended approximately normal to the plane of the bilayer (Fig. 2) changes steadily from that expected from a well ordered hexagonal lattice of chains with a well defined sharp Bragg reflection at 1/4. 15 Å $[(2\sin\theta)/\lambda]$ with little off-equatorial spreading for dipalmitoyl phosphatidylcholine alone to that expected for a statistically disordered amorphous packing of the chains [20] with a broad reflection at 1/4. 25 Å and considerable broad off-equatorial diffraction at the highest level of chlorophyll incorporation. The statistically disordered amphorous chain packing has been described by us previously and arises from lattice disorder coupled with substitution disorder [21] when chains of a significantly different composition, such as branched hydrocarbon chains (e.g. isoprenoid chains) as opposed to normal fatty-acid chains, are incorporated into dipalmitoyl phosphatidylcholine bilayers without a lateral phase separation [22] of the two components. Hence, as chlorophyll is increasingly incorporated into the dipalmitoyl phosphatidylcholine bilayer, the average separation between chains and the degree of statistical disorder in the packing of chains in the plane of the bilayer increases. However, these changes in chain packing in the plane of the bilayer do not significantly alter the electron density profile structure $\mu(x)$ (as seen in $\Delta\mu(x)$ in the hydrocarbon core of the bilayer, i.e. $\mu(-16\,\text{Å} \leqslant x \leqslant 16\,\text{Å})$, as identified for dipalmitoyl phosphatidylcholine alone previously by us [7]. The increased average separation of chains and increased disorder in their packing in the plane of the hydrocarbon core of the bilayer without a decrease in the width of the hydrocarbon core and/or a significant change in its profile structure can best be explained by a penetration of the chlorophyll phytol chains in a relatively extended form between the fatty-acid chains of the host phosphatidylcholine without a lateral phase separation of the two components (note that the lengths of extended palmitate and phytol chains are nearly equal). These results are not likely to be explained by even a small penetration of the chlorophyll porphyrin ring into the hydrocarbon core of the lipid bilayer as demonstrated previously by us using fluorescent probe molecules with even smaller aromatic ring structures [6, 7].

(b) The significantly increased width and less sharp features of the polar headgroup region in the electron density profile structure of the bilayer $\mu(17\,\text{Å} \leqslant |x| \leqslant 28\,\text{Å})$, as identified by us previously [7], with increasing chlorophyll incorporation (as seen in Fig. 5) can be qualitatively explained by the added presence of a rather constant relatively high electron density step function of width 8 Å in that region as expected for the chlorophyll porphyrin ring in the profile projection at this resolution with an inclination of about 54° to the plane of the bilayer.

(c) We note that the results from absorption polarization spectroscopy would also be consistent with an isotropic distribution of chlorophyll porphyrin orientations in the polar headgroup region of the bilayer. However, the width of the polar headgroup layer, the unperturbed hydrocarbon core of the profile structure and the close proximity of the adjacent bilayer membrane in the multilayer at maximal chlorophyll incorporation would seem to rule out this possibility.

Hence, (a), (b) and (c) above justify our above stated model for chlorophyll

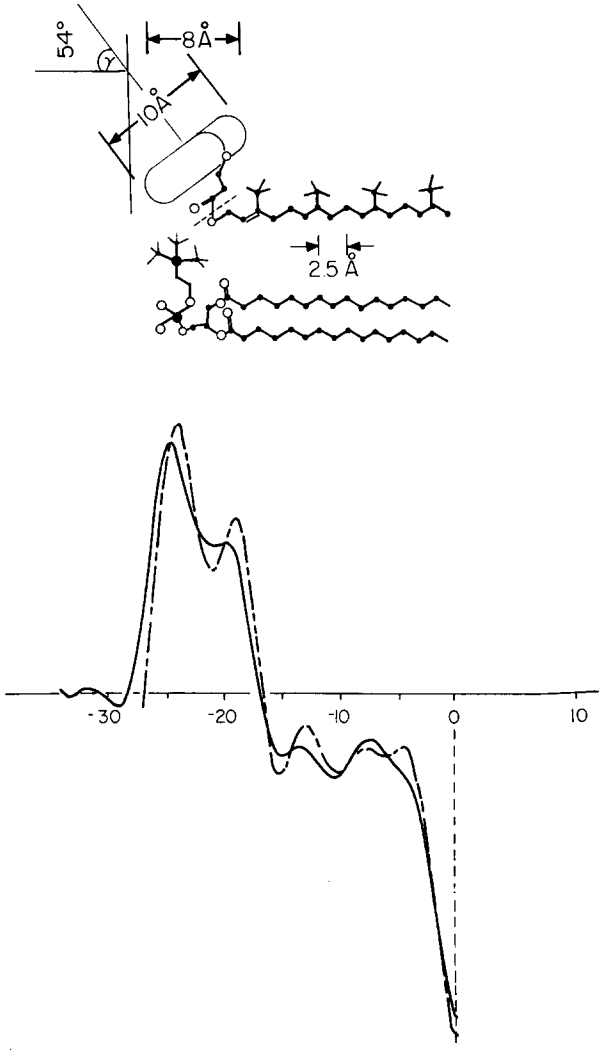

location in the dipalmitoyl phosphatidylcholine bilayer membrane below the thermal phase transition of the phosphatidylcholine fatty-acid chains. The proposed model is shown schematically above; (– – –) dipalmitoyl phosphatidylcholine, (—) dipalmitoyl phosphatidylcholine/chlorophyll. A more quantitative fit of the proposed model to the calculated profile projection does not seem justified at this time since the area per molecule in the mixed bilayer and the water distribution profile in the polar headgroup region of the mixed bilayer are not known.

DISCUSSION: NUCLEAR MAGNETIC RESONANCE

Phytol and bacteriochlorophyll solution in C^2HCl_3

The question has been raised as to whether all the bacteriochlorophylls are esterified at the propionic acid level by phytyl chains. Katz et al. [24] have

recently reported that the chlorophyll extracted from the purple photosynthetic bacteria *R. rubrum* is esterified by all-*trans* geranyl-geraniol (four double bonds). On the other hand, Rapoport and Hamlow [25] have shown that the chlorophyll from *Chlorobium thiosulphatophilum*, a green photosynthetic bacterium, is esterified by all-*trans* farnesol (three saturated bonds along the chain). Our NMR results on the C^2HCl_3 solution of bacteriochlorophyll from the green mutant of *R. Sphaeroides* (a purple bacterium) have indicated the presence of esterifying phytyl chains.

Dipalmitoyl phosphatidylcholine/chlorophyll and dipalmitoyl phosphatidylcholine/phytol vesicles in water.

The location of chlorophyll in the mixed bilayer. The upfield chemical shifts induced in the resonance of the phosphatidylcholine $N^+(CH_3)_3$, *N*-methylene and chain methylene groups in the 2-position by incorporation of chlorophyll into the dipalmitoyl phosphatidylcholine bilayers are interpreted as due to local diamagnetic anisotropy effects [26] produced by the porphyrin rings in the vicinity of neighboring phosphatidylcholine proton groups. The strength of the "ring current" effects depend on the area of the ring, while the intensity and orientation of the induced local magnetic field vectors vary with the distance from the center and the azimuthal angle with respect to the plane of the ring. Quantitative calculations of the field generated by the porphyrin rings of a chlorophyll molecule are difficult because of the lack of a completely satisfactory treatment of the diamagnetic anisotropy of conjugated multiring systems, especially in the presence of various substituents. However, the fact that the ring diamagnetic anisotropies are typically able to create only short range effects limited to a few Ångstroms strongly suggests that the porphyrin rings are located in the bilayer in the region of the polar headgroups. The fact that the choline $N^+(CH_3)_3$ resonance in dipalmitoyl phosphatidylcholine/chlorophyll vesicles is clearly composed of two peaks both of which are shifted upfield on chlorophyll incorporation indicates that chlorophyll is incorporated on both sides of the bilayer and also that a slightly different molecular packing exists at the level of the phosphatidylcholine headgroups on the two vesicle surfaces.

The fact that the linewidths of the choline *N*-methyl signals are only slightly affected by phytol and chlorophyll introduction indicates that the average vesicle size is probably about the same in these systems; therefore the different selective linebroadenings observed in the resonances of the chains (methylene and methyl groups) are due to different local dynamical structures dominating the dynamical packing in the hydrophobic cores of the bilayers. In particular the chain methylene signal is much broader in dipalmitoyl phosphatidylcholine/phytol than in dipalmitoyl phosphatidylcholine/chlorophyll and both are much broader than in pure dipalmitoyl phosphatidylcholine vesicles. The difference in resonance linewidths between the two former systems cannot be ascribed to different vesicle sizes, because the choline *N*-methyl signal show not only less dramatic line broadenings, but even linebroadenings opposite in sign to those exhibited by chain methylene resonances. These results along with those of the preceeding paragraph suggest that the observed selective modifications of chain resonance linewidths are related to the incorporation of the phytyl chains into the hydrophobic core of the phosphatidylcholine bilayer. Different dynamical packings are shown to exist according to whether phytyl chains are introduced as such or as esterifying alcohols of chlorophyll molecules.

In addition, spin-lattice relaxation times may provide further information regarding the localization of the porphyrin rings within the polar headgroup level of the mixed bilayer; the choline *N*-methyl T_1 relaxation rates are only slightly affected by the incorporated phytol, but strongly incremented by the presence of the porphyrin rings of the incorporated chlorophyll. However, it has been shown by NMR studies carried out in this laboratory on phosphatidylcholine bilayers incorporating fluorescent probe molecules that the modification in T_1 exhibited by the various phosphatidylcholine proton groups is not necessarily strictly confined to the local region in which the probe is located [27].

In conclusion, the parallel use of phytol and chlorophyll for T_1 and $\Delta\nu_{\frac{1}{2}}$ measurements together with the utilization of the described "ring current" effects seems able to meaningfully restrict the possible interpretations and lead to a rather clear model for the location of chlorophyll within the phosphatidylcholine bilayer structure.

The intramolecular dynamics of phosphatidylcholine and chlorophyll in the mixed bilayer. Unlabeled chlorophyll *a* and [^{2}H]chlorophyll *a* have identical effects in enhancing the T_1 relaxation rate of the phosphatidylcholine *N*-methyl groups indicating that intermolecular magnetic dipole-dipole interactions with the chlorophyll porphyrin rings are ineffective in their T_1 relaxation. It has been shown by us in previous T_1 relaxation studies carried out at different frequencies on phosphatidylcholine vesicles [19], that the spin-lattice relaxation values of the choline *N*-methyl group and of several proton groups along the phosphatidylcholine molecule are determined by a more than one-correlation-time mechanism of intramolecular motion. According to Woessner's model, rotation about single bonds and reorientation of the axis about which rotation occurs can provide a mechanism for such spin-lattice relaxation [28, 29]. The enhanced T_1 rates exhibited by the choline *N*-methyl groups upon chlorophyll introduction in the bilayer might be related to changes induced in the correlation times of these intramolecular motions, in particular to an increase in the rotational correlation time about the N–C bonds and/or a decrease in the reorientational correlation time of the N–C bond axis. However, incremented intermolecular magnetic dipole interactions among dipalmitoyl phosphatidylcholine molecules could also explain the T_1 rate enhancement.

The T_1 relaxation times of the methylene groups of the chains in the dipalmitoyl phosphatidylcholine/phytol and dipalmitoyl phosphatidylcholine/chlorophyll mixed bilayers appear identical to that shown by pure dipalmitoyl phosphatidylcholine vesicles. The result does not necessarily indicate an unaltered phosphatidylcholine chain mobility in the hydrocarbon core of the bilayer: in fact, it is necessary to point out that the chain methylene resonance is composed of contributions by both the phosphatidylcholine and the phytol protons in these cases. Moreover, strong modifications in the mobility of all the chains was indicated by the induced line-broadening of these resonances upon phytol and chlorophyll incorporation as already discussed. The fact that phytol and chlorophyll have the same effect on T_1 relaxation of the methylene groups of the chains while phytol has a greater effect on the resonance linewidth offers a further indication that different motions must determine T_1 and resonance linewidth in these systems. In agreement with the conclusion obtained from the analysis of the temperature and frequency dependence of T_1 relaxation times in pure dipalmitoyl phosphatidylcholine bilayers [19], T_1 and resonance linewidth measurements are reconciled by considering different degrees

of anisotropy in chain methylene group motion induced by the two molecules. (It should be noted here that recent proton magnetic relaxation measurements (T_1 and T_2) in our laboratory on mixed phosphatidylcholine bilayer membranes in the form of sonicated single-wall vesicles of similar size show that the linewidth of the chain methylene group resonance band is predominately due to T_2 relaxation.) The results obtained on analysing the magnetic relaxation of the chain methylene resonances in this manner suggest that the reorientational motions of the axes about which the chain methylene groups rotate are much slower than the rotations themselves in both the phytol and chlorophyll-incorporated systems so that the total contribution of the reorientational motions to T_1 relaxation is practically negligible. Within this interpretation, the reorientational correlation time appears longer in the case of phytol relative to chlorophyll incorporation resulting in the larger linewidth observed for the methylene resonance of the chains.

The behavior of the spin-lattice relaxation of the terminal and side-chain methyl groups of the chains in dipalmitoyl phosphatidylcholine/phytol and in dipalmitoyl phosphatidylcholine/chlorophyll *a* mixed bilayers appears analogous to that of the chain methylene groups in several respects with the complication that the restricted rotation of the side-chain methyl groups along the phytyl chains is a further explanation for enhancement of the total relaxation rate. In particular the T_1 rate values of the methyl groups in the system dipalmitoyl phosphatidylcholine/[^{2}H]-chlorophyll *a* as compared to those of pure dipalmitoyl phosphatidylcholine vesicles indicate that at the level of the terminal methyl groups the rotational mobility of the phosphatidylcholine chains is rather severely restricted in the presence of the chlorophyll phytyl chains. This can be reasonably attributed to the presence of the chlorophyll phytyl chains, and in particular to their cumbersome side-chains methyl groups. These lateral methyl groups, in turn, are provided with higher rotational mobility than that of the phosphatidylcholine terminal methyl groups as seen by comparing the relaxation rates of the methyl groups in dipalmitoyl phosphatidylcholine/chlorophyll *a* to those in dipalmitoyl phosphatidylcholine/[^{2}H]chlorophyll *a*.

The contributions to the relaxation rates of the dipalmitoyl phosphatidylcholine chains alone in the mixed bilayers can be isolated by introducing fully deuterated chlorophyll into the bilayers. The temperature behavior of T_1 relaxation measured for the chain methylene groups from the C_4 to the C_{15} positions indicate for these proton groups the lack of the "extreme narrowing conditions" for the fastest motion responsible for their spin lattice relaxation (see also the second paragraph above). This indicates that the correlation time of the rotation around the C-C bonds is larger than 10^{-9}–10^{-10} s in the temperature range investigated. An attempt to isolate the contributions of the spin-lattice relaxation, due to the phytyl and phosphatidylcholine methylene groups, has been carried out under the assumption that the contributions to relaxation due to intermolecular phosphatidylcholine-phosphatidylcholine and phosphatidylcholine-chlorophyll interactions can be neglicted with respect to the intramolecular terms. This hypothesis has been essentially verified in dipalmitoyl phosphatidylcholine/fatty-acid mixed bilayers in so far as the temperature is maintained several degrees above the thermal phase transition [31]. The T_1 relaxation values for the phytyl chain methylene (and -CH) groups (T_{1Ph}) have been determined using the relation:

$$e^{-t/(T_1)} = f_{DPPC}\, e^{-t/(T_1)^2H} + f_{Ph}\, e^{-t/(T_1)Ph}$$

where (T_1) is the T_1 value measured in the system dipalmitoyl phosphatidylcholine/chlorophyll *a*, and $(T_1)^2H$ the value determined in dipalmitoyl phosphatidylcholine/[^{2}H]chlorophyll *a*; f_{DPPC} and f_{Ph} are respectively the proton fractions "seen" along the dipalmitoyl phosphatidylcholine and the phytyl chains in the dipalmitoyl phosphatidylcholine/chlorophyll *a* system. As already mentioned (Results Section), practically all the protons of the phytyl chains contribute to the high resolution spectrum while only 58 % of the protons of the dipalmitoyl phosphatidylcholine chains are contributing to the methylene and methyl resonances at 70 °C and about 40 % at 53 °C. For the calculations the assumption has been made that similar proton fractions apply also to the chain methylene resonance band alone, a reasonable first approximation considering that the methylene resonance is predominant among the fatty-acid chain proton resonances. The plots of Fig. 11 indicate that in contrast to the restricted rotational mobility of the host phosphatidylcholine chains, the phytyl chains show a high degree of mobility in the bilayer, their hindered rotation about the C-C bonds occurring with correlation times less than 10^{-9}–10^{-10} s. It is interesting to note that such different relaxation contributions of the two components, phosphatidylcholine and chlorophyll, are compensated in the system dipalmitoyl phosphatidylcholine/chlorophyll *a* to give a resulting average T_1 relaxation behaviour very close to that of pure dipalmitoyl phosphatidylcholine vesicles.

Finally the effect of bacteriochlorophyll on the spin-lattice relaxation rates in these mixed model membranes appears in general considerably different from that of chlorophyll *a*. The lack of parallel differences in the resonance linewidths indicate that the longer-correlation time motions, such as the reorientation of the bond rotation axes, must be substantially the same. The differences observed in the T_1 relaxation values and in the slopes of their log plots vs reciprocal temperature can be therefore mainly attributed to differences in the rotational activation energies about single bonds. It appears difficult at this stage to indicate the reasons why two types of chlorophyll, both apparently esterified by phytyl chains, are able to induce different dynamic

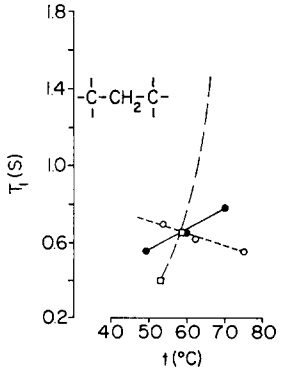

Fig. 11. Proton spin-lattice relaxation time T_1 as a function of temperature for the average chain methylene group for (○) dipalmitoyl phosphatidylcholine chains (measured) and (□) phytyl chains (calculated), and (●) both (measured) averaged together in a mixed bilayer at a molar ratio of dipalmitoyl phosphatidylcholine/chlorophyll *a* of 3 : 1.

structures in the bilayers. The consideration of the differences in the molar ratios dipalmitoyl phosphatidylcholine/chlorophyll used in the two systems does not seem to be sufficient to explain these differences in T_1 relaxation: simply on the basis of concentration we should expect less perturbed relaxation rates in dipalmitoyl phosphatidylcholine/bacteriochlorophyll than in dipalmitoyl phosphatidylcholine/chlorophyll *a* with respect to pure dipalmitoyl phosphatidylcholine vesicles while the opposite situation is observed. At this stage different substituents on the chlorophyll porphyrin rings appear to be able to affect differently the dynamic structure of a phosphatidylcholine model membrane, directly and/or indirectly.

CONCLUSIONS

Our results from structural and dynamic studies on dipalmitoyl phosphatidylcholine bilayers incorporated with chlorophyll both below and above the thermal phase transition of the fatty-acid chains of the host phosphatidylcholine show that:

(1) Chlorophyll is incorporated into the phosphatidylcholine bilayer with its porphyrin ring located anisotropically in the polar headgroup layer of the membrane and with its phytol chain in a relatively extended form between the phosphatidylcholine fatty-acid chains in the hydrocarbon core of a mixed bilayer membrane.

(2) The intramolecular anisotropic rotational dynamics of the host phosphatidylcholine molecules are significantly perturbed upon chlorophyll incorporation into the bilayer at all levels of the phosphatidylcholine structure. These dynamics for the host phosphatidylcholine fatty-acid chains are qualitatively different from that of the incorporated chlorophyll phytol chains on a 10^{-9}–10^{-10} s time scale in the ideally mixed two-component bilayer.

Our conclusions with regard to chlorophyll location in the host phosphatidylcholine bilayer are similar to those of Cherry et al. [23] derived from electrical and optical studies. It is of interest to note that the bacteriochlorophyll absorption spectra and the angle of the bacteriochlorophyll porphyrin ring inclination to the bilayer plane remains constant over the range of relative concentrations of bacteriochlorophyll/dipalmitoyl phosphatidylcholine investigated. In addition, the porphyrin ring inclination angle to the bilayer plane determined here for the mixed bilayers in close apposition in the oriented multilayer is similar to that found by others [23] for widely separated or single mixed bilayers. These results suggest that the chlorophyll porphyrin ring inclination in these systems is primarily a function of chlorophyll-phosphatidylcholine interactions in the bilayer structure and not chlorophyll aggregation in the plane of the mixed bilayer or chlorophyll-chlorophyll interactions between adjacent bilayers in the multilayer.

ACKNOWLEDGEMENT

This work has been supported by the research grants NIH-GM12202 and NSF-GB32407.

REFERENCES

1 Cain, J. E. and Blasie, J. K. (1972) Biophys. J. 12, 45a
2 Podo, F. and Blasie, J. K. (1973) Biophys. J. 13, 251a
3 Smith, J. H. and Benitez, A. (1955) Moderne Methoden der pflanzenanalyse (Paech, K. and Tracey, M. V., eds), Vol. IV, Springer-Verlag, Berlin
4 Kim, W. S. (1966) Biochim. Biophys. Acta 112, 392–402
5 Lesslauer, W. and Blasie, J. K. (1972) Biophys. J. 12, 175–190
6 Lesslauer, W., Cain, J. and Blasie, J. K. (1971) Biochim. Biophys. Acta 241, 547–556
7 Lesslauer, W., Cain, J. E. and Blasie, J. K. (1972) Proc. Natl. Acad. Sci. U.S. 69, 6 1499–1503
8 Farrar, T. C. and Becker, E. D. (1971) Pulse and Fourier Transform NMR, Academic Press, New York
9 Gillies, D. G. and Shaw, D. (1972) The Application of Fourier Transformation to High Resolution Nuclear Magnetic Resonance Spectroscopy, Annual Reports of NMR (Mooney, ed.), Vol. 5, Academic Press New York
10 McDonald, G. G. and Leigh, Jr., J. S. (1973) J. Magn. Resonance 9, 358–362
11 Lesslauer, W. and Blasie, J. K. (1971) Acta Crystallogr. A27, 456–461
12 "High Resolution NMR Spectra Catalog" (1962) Varian Associates, Palo Alto, California (a) Spectrum 346, (b) Spectrum 279
13 Bates, R. B. and Gale, D. M. (1960) J. Am. Chem. Soc. 82, 5749–5751
14 Gale, P. H., Arison, B. H., Trenner, N. R., Page, Jr., A. C. and Folkers, K. (1963) Biochemistry 2, 196–200
15 Closs, G. L., Katz, J. J., Pennington, F. C., Thomas, M. R. and Strain, H. H. (1963) J. Am. Chem. Soc. 85, 3809–3821
16 Katz, J. J., Dougherty, R. C. and Boucher, L. J. (1966) The Chlorophylls (Vernon, L. P. and Seeley, G. R., eds), pp. 186, Academic Press, New York
17 Lee, A. G., Birdsall, N. J. M., Levine, Y. K. and Metcalfe, J. C. (1972) Biochim. Biophys. Acta 255, 43–56
18 Kostelnik, R. J. and Castellano, S. M. (1973) J. Magn. Resonance 9, 291–295
19 McLaughlin, A., Podo, F. and Blasie, J. K. (1973) Biochim. Biophys. Acta 330, 109–121
20 Hosemann, R. and Bagchi, S. N. (1966) Direct Analysis of Diffraction by Matter, North-Holland Publishing Company, Amsterdam
21 Cain, J., Santillan, G. and Blasie, J. K. (1972) in Membrane Research (Fox, C. F., ed.) Academic Press, New York
22 McConnell, H. M., Devaux, P. and Scandella, C. (1972) in Membrane Research, pp. 27–37 (Fox, C. F., ed.), Academic Press, New York
23 Cherry, R. J., Hsu, K. and Chapman, D. (1972) Biochim. Biophys. Acta 267, 512–522
24 Katz, J. J., Strain, H. H., Harkness, A. L., Studier, M. H., Svec, W. A., Janson, T. R. and Cope, B. T. (1972) J. Am. Chem. Soc. 94, 7938–7939
25 Rapoport, H. and Hamlow, H. P. (1961) Biochem. Biophys. Res. Commun. 6, 134–137
26 Jackman, L. M. and Sternell, S. (1969) Applications of Nuclear Magnetic Resonance Spectroscopy in Organic Chemistry, Pergamon Press, Oxford
27 Podo, F. and Blasie, J. K. (1975) Proc. Natl. Acad. Sci. U.S., in the press
28 Woessner, D. E. (1962) J. Chem. Phys. 36, 1–4
29 Woessner, D. E. (1962) J. Chem. Phys. 37, 647–654
30 Goldman S. (1953) Information Theory, Prentice-Hall, New York
31 Podo, F. and Blasie, J. K. (1976) Biochim. Biophys. Acta 419, 1–18